

# Kinetics of the Thermal Desorption of Atomic Oxygen during Transformations $\text{BiO}_{2-x} \rightarrow \beta\text{-Bi}_2\text{O}_3 \rightarrow \alpha\text{-Bi}_2\text{O}_3$

A. N. Romanov, Z. T. Fattakhova, Yu. N. Rufov, and D. P. Shashkin

*Semenov Institute of Chemical Physics, Russian Academy of Sciences, Moscow, 117977 Russia*

Received January 18, 1999

**Abstract**—The thermal desorption of atomic oxygen during the transformations  $\text{BiO}_{2-x} \rightarrow \beta\text{-Bi}_2\text{O}_3 \rightarrow \alpha\text{-Bi}_2\text{O}_3$  is shown to be due to the removal of overstoichiometric oxygen from the bulk of  $\beta\text{-Bi}_2\text{O}_3$ . Oxygen formed at the first stage is desorbed in a molecular form. The maximum desorption rate of atomic oxygen is found before the phase transformation  $\beta\text{-Bi}_2\text{O}_3 \rightarrow \alpha\text{-Bi}_2\text{O}_3$ . The activation energy of the diffusion of excess oxygen in the  $\beta\text{-Bi}_2\text{O}_3$  lattice is  $\approx 30$  kcal/mol.

## INTRODUCTION

“Active” oxygen is given special attention in the mechanistic studies of the selective oxidation of hydrocarbons on mixed-oxide catalysts, and the nature of this species is still under discussion. Various oxygen species on the surface of metal oxides are known:  $\text{O}^-$ ,  $\text{O}^{2-}$ ,  $\text{O}_2^{\text{ads}}$ ,  $\text{O}_2^-$ ,  $\text{O}_2^{3-}$ ,  $\text{O}_3^-$ , and  $\text{O}_4^-$  [1]. When oxygen desorbs, the species become less diverse. The desorption of the  $\text{O}$ ,  $\text{O}_2$ ,  $^1\Delta_g \text{O}_2$ , and  $\text{O}_3$  species was found under different conditions [2–4]. The nature of desorbed oxygen species should be taken into account in studies of heterogeneous–homogeneous catalytic processes. This is also important for the so-called remote-control mechanism that was suggested to account for the effect of synergism on multiphase catalysts for partial oxidation. This effect manifests itself in that active species are formed on some regions of a catalyst and react on other regions.

It was found in a series of studies that some oxides (for example,  $\text{Bi}_2\text{O}_3$ ,  $\text{Sb}_2\text{O}_4$ , etc.) play a role of active oxygen donors, whereas other oxides are oxygen acceptors, and the catalytic process occurs on the latter oxides (see, for instance, [5]). It was shown in [6] that active oxygen, which participates in the reaction, comes from the bulk of the donor oxide and the gaseous oxygen becomes active only after passing through the volume of a grain of the donor oxide. Therefore, the study of the properties of active oxygen and the conditions of its diffusion from the grain bulk to the surface and migration to catalytic sites is especially important. In our previous study [7], we carried out a simulation of oxygen migration from the grain bulk to the surface and proposed a model to determine the diffusivity. It was found that the oxygen atom is a possible species of active oxygen, which can be monitored as  $\text{O}_3$  when  $\text{O}_2$  is present in the gas phase.  $\text{O}_3$  is formed from  $\text{O}$  via the

fast reaction  $2\text{O}_2 + \text{O} \rightarrow \text{O}_3 + \text{O}_2$ . The reaction  $\text{O}_2^{\text{g}} + \text{O}^{\text{ads}} \rightarrow \text{O}_3^{\text{g}}$  was ruled out for the following reason. According to the reported data [1], a precursor of  $\text{O}_3^-$  decomposes on the oxides under study at  $T > 150^\circ\text{C}$ . In our experiments, desorption occurs at  $T > 300^\circ\text{C}$  and reaches a maximum in the range  $400\text{--}500^\circ\text{C}$ , and this likely eliminates the possibility of the above reaction.

This work is intended to find a relationship between the genesis of bismuth oxide, a component of multi-component catalysts for the partial oxidation of hydrocarbons, and the kinetics of oxygen thermal desorption in both molecular and atomic forms. To our knowledge, such studies were not carried out earlier.

## EXPERIMENTAL

Samples of  $\text{BiO}_{2-x}$  were prepared by the oxidation of bismuth hydroxide with sodium persulfate (sample 1) or potassium ferricyanide (sample 2) in an alkali solution.

Samples of  $\beta\text{-Bi}_2\text{O}_3$  were prepared by three procedures: the heating of  $\text{BiO}_{2-x}$  (sample 1) at  $350^\circ\text{C}$  for 10 min (sample 3), the heating of basic bismuth carbonate ( $\text{Bi}_2\text{O}_2\text{CO}_3$ ) at  $380^\circ\text{C}$  for 20 min (sample 4), and the treating of a solution of bismuth nitrate with excess 2 mol/l solution of sodium hydroxide at  $100^\circ\text{C}$  for 3 min followed by fast filtration of a precipitate and thorough washing (sample 5). The latter sample differs from more fine-crystalline samples 3 and 4 by stability on exposure to  $\text{H}_2\text{O}$  and  $\text{CO}_2$ . For more detailed data on the preparation of these samples, see [8].

Hydrated  $\beta\text{-Bi}_2\text{O}_3$  (sample 6) was prepared by storing fine-crystalline  $\beta\text{-Bi}_2\text{O}_3$  (samples 3 and 4) in wet air for several days or by the impregnation of the samples with water followed by fast drying at  $120^\circ\text{C}$ .

The thermal desorption of atomic oxygen (ozone) was measured by chemiluminescence in an air flow as described in [9]. A signal from a selective amplifier was recorded using a Pentium-based PC via a 12-bit analog-to-digital converter using original software for recording and treating the signals.

The thermal desorption of molecular oxygen was studied in a helium flow under the conditions of a linear increase in temperature at a rate of 10°C/min. Desorbing water and CO<sub>2</sub> were collected in a silica gel trap. Evolved oxygen was recorded with a thermal-conductivity detector.

X-ray diffraction analysis was performed using a DRON-3 instrument (CuK<sub>α</sub>-irradiation).

DTA and DTG curves were recorded using an MOM analyzer (Hungary).

The experiments in an isothermal regime were carried out as follows: a sample was introduced into the reactor preheated to a specified temperature; purging with air and O<sub>3</sub> recording were not interrupted during these experiments.

The experimental thermal desorption curves obtained in the isothermal regime were approximated by the  $\exp(-kt)$  or  $\exp(-k\sqrt{t})$  functions. Experimental data fit was worse if other functions were used. A criterion for the best fit was the minimum root-mean-square deviation of the experimental data from the calculated curve. The desorption rates thus calculated at different temperatures obey the Arrhenius equation, from which the activation energy of the process was found.

## RESULTS

The X-ray diffraction study showed the correspondence of the spectra for BiO<sub>2-x</sub> and β-Bi<sub>2</sub>O<sub>3</sub> to the tabulated values for these substances. Samples 1 and 2 prepared by different procedures were crystallographically identical (fluorite-type cubic lattice).

The thermogravimetric measurements revealed a marked weight change in the range of 340–380°C and a small endothermic peak at 380°C, which, according to the reference data, indicates the decomposition of BiO<sub>2-x</sub> to β-Bi<sub>2</sub>O<sub>3</sub>. A small exothermic peak at  $\approx$ 530°C appeared on further heating at almost constant weight, which we attributed to the β-Bi<sub>2</sub>O<sub>3</sub>  $\rightarrow$  α-Bi<sub>2</sub>O<sub>3</sub> transition.

Essential weight variations were not found on the DTA curve of the β-Bi<sub>2</sub>O<sub>3</sub> sample. The DTA curve has a small exothermic peak at 420°C, which corresponds to the β-Bi<sub>2</sub>O<sub>3</sub>  $\rightarrow$  α-Bi<sub>2</sub>O<sub>3</sub> transition and is in good agreement with the reported data. The origin of the somewhat enhanced temperature of the phase transition in the case of β-Bi<sub>2</sub>O<sub>3</sub> prepared by the decomposition of BiO<sub>2-x</sub> remains unclear. In this case, β-Bi<sub>2</sub>O<sub>3</sub> is likely stabilized by the hydroxyl groups that were introduced into BiO<sub>2-x</sub> during preparation in an aqueous

solution or by excess lattice oxygen, which was not removed completely upon dioxide decomposition.

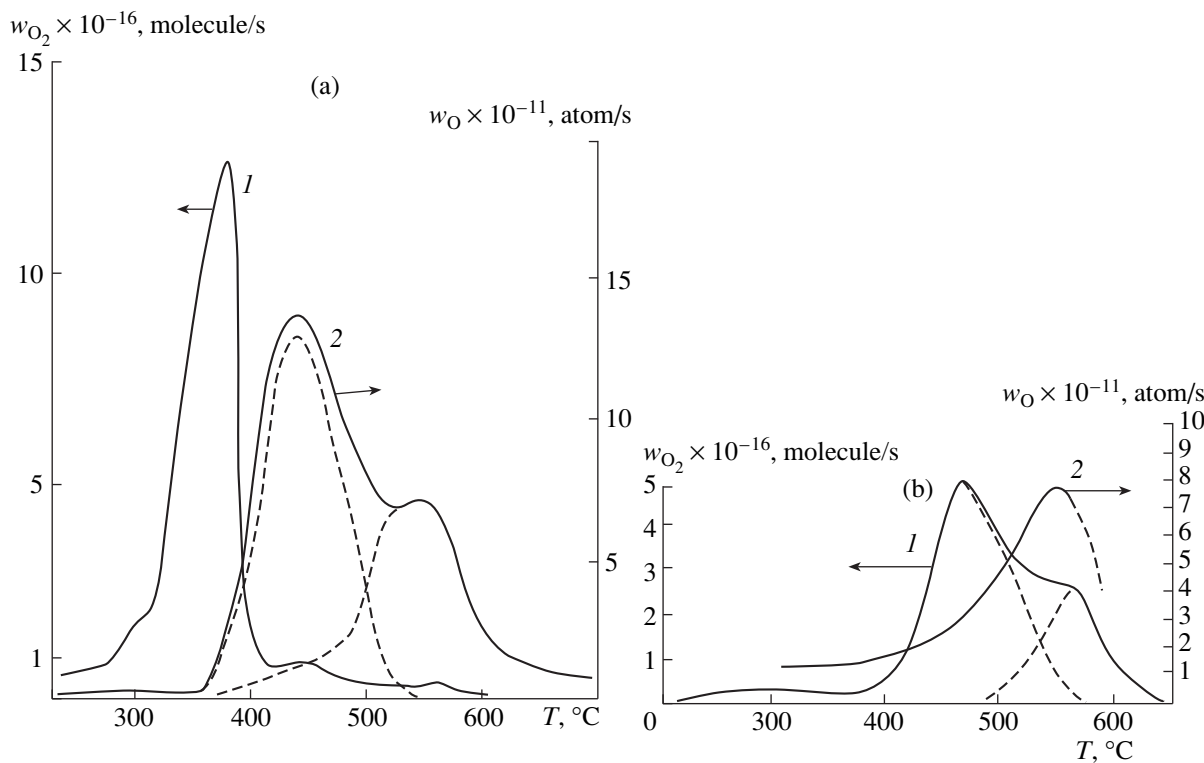
Figure 1 presents the experimental thermal desorption curves both for O<sub>2</sub> and O, which was monitored as O<sub>3</sub> for the BiO<sub>2-x</sub> and β-Bi<sub>2</sub>O<sub>3</sub> samples. The maximum temperature of O<sub>2</sub> thermal desorption from the BiO<sub>2-x</sub> sample coincides with that for BiO<sub>2-x</sub> decomposition to β-Bi<sub>2</sub>O<sub>3</sub>. In addition, two small peaks at  $\approx$ 445 and 560°C appeared with an increase in temperature. The thermal desorption of atomic oxygen during the BiO<sub>2-x</sub> decomposition is at the background level, then it sharply increases after passing through maximum of decomposition, and reaches a maximum (437°C) somewhat earlier than the second maximum at 445°C appears on the thermal desorption curve for O<sub>2</sub>.

Table 1 lists the main parameters of oxygen thermal desorption for the samples under study. Note the amount of oxygen that evolved during BiO<sub>2-x</sub> decomposition and was estimated from the thermal desorption data is in good agreement with the DTA findings for the oxygen-deficient BiO<sub>2-x</sub> dioxide (parameter x depends on the preparation procedure and achieves values up to 0.25). The amount of atomic oxygen evolved during the BiO<sub>2-x</sub>  $\rightarrow$  Bi<sub>2</sub>O<sub>3</sub> transition is  $\approx$ 10<sup>-6</sup> of the amount of desorbed molecular oxygen.

The preparation procedure for the BiO<sub>2-x</sub> samples does not actually affect the experimental results. Only slight differences were found in the temperatures of phase transition and the amount of desorbed oxygen (because of different oxygen concentration in the non-stoichiometric BiO<sub>2-x</sub>).

In the case of preliminarily prepared β-Bi<sub>2</sub>O<sub>3</sub>, the low-temperature peak (375°C) due to the evolution of molecular oxygen via the reaction BiO<sub>2-x</sub>  $\xrightarrow{-O_2}$  β-Bi<sub>2</sub>O<sub>3</sub> is absent but the high-temperature maxima at 445 and 560°C are still present. These peaks on the thermal desorption curve are likely due to the removal of overstoichiometric lattice oxygen from the β-Bi<sub>2</sub>O<sub>3</sub> lattice rather than the decomposition of bismuth dioxide. Apparently, these processes also produce atomic oxygen during thermal desorption (the maximum of evolution is seen at  $\approx$ 540°C). β-Bi<sub>2</sub>O<sub>3</sub> prepared by bismuth dioxide decomposition contains a significant amount of overstoichiometric oxygen. The results of thermal desorption measurements show that the oxygen concentration corresponds to the β-Bi<sub>2</sub>O<sub>3.16</sub>. Meanwhile, the data of X-ray diffraction study of nonstoichiometric samples are the same as the data for usual β-Bi<sub>2</sub>O<sub>3</sub>. This fact is due to the presence of oxygen vacancies in the β-Bi<sub>2</sub>O<sub>3</sub> lattice, which are capable of accepting excess oxygen without reconstruction of the crystal lattice.

To study desorption kinetics in more detail, we performed experiments in the isothermal regime. Measurements were conducted at various temperatures with a fresh sample in each run. Table 2 presents the results of experiments on atomic oxygen desorption in the isothermal regime. The exponential kinetics for thermal



**Fig. 1.** Thermal desorption of (1)  $O_2$  and (2) O from (a)  $BiO_{2-x}$  (sample 2) and (b)  $\beta$ - $Bi_2O_3$  (as-prepared sample 3).  $w$  is the thermal desorption rate. The dashed line shows deconvolution to distinct peaks.

desorption decay was found for two samples, hydrated bismuth oxide (sample 6) and fine-crystalline  $\beta$ - $Bi_2O_3$  (sample 4). A more complicated time profile of the rate of atomic oxygen evolution was found for sample 5 prepared by precipitation with alkali. This fact will be discussed below.

Figure 2 shows the decay curves for atomic oxygen desorption at different temperatures. The two-peak pattern is clearly seen, which can be explained by the desorption of the surface oxygen (the first peak) and the subsequent desorption of oxygen, which diffuses from the bulk (the second peak).

We also studied ozone decay both on the reactor walls and on the oxide samples. The concentrations of atomic species and ozone presented in the table are underestimated because of the decay on both the samples and reactor walls. Nevertheless, different samples and the concentrations in two peaks for the same sample can be compared semiquantitatively.

## DISCUSSION

The experimental results for the thermal decomposition of  $BiO_{2-x}$  (Table 1, samples 1 and 2) provide evidence that atomic oxygen is formed beginning from  $T > 360^\circ C$  and up to the temperature of  $\beta$ - $Bi_2O_3 \rightarrow \alpha$ - $Bi_2O_3$  phase transition. Because only  $\beta$ - $Bi_2O_3$  exists in this temperature range during decomposition, atomic

oxygen is likely formed from overstoichiometric lattice oxygen of the  $\beta$ -phase, which diffuses from the bulk to the surface. After the removal of excess lattice oxygen (which stabilizes  $\beta$ - $Bi_2O_3$ ), the  $\beta$ - $Bi_2O_3 \rightarrow \alpha$ - $Bi_2O_3$  transition occurs.

**Table 1.** Thermal desorption of molecular and atomic oxygen from bismuth oxides

Sample	$S_{sp}$ , $m^2/g$	$O_2$		O	
		amount of desorbed molecules, $g^{-1}$	temperature of the desorption maximum, $^\circ C$	amount of desorbed atom, $g^{-1}$	temperature of the desorption maximum, $^\circ C$
1	3.5	$3 \times 10^{20}$	365	$1.7 \times 10^{14}$	470
		—	475	$2.0 \times 10^{14}$	510
2	4.3	$4.2 \times 10^{20}$	375	$4.4 \times 10^{14}$	437
		$9.5 \times 10^{17}$	445	$5.0 \times 10^{14}$	545
3	15.6	$1.4 \times 10^{20}$	445	$2.0 \times 10^{15}$	540
		—	560	—	—
4	3.8	—	—	$4.4 \times 10^{13}$	545
5	0.7	—	—	$1.8 \times 10^{13}$	340

The chemical reaction  $\text{BiO}_{2-x} \rightarrow \beta\text{-Bi}_2\text{O}_3$ , which produces the main amount of molecular oxygen, does not lead to the additional desorption of atomic oxygen.

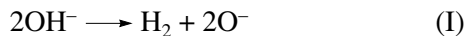
The model of a “black sphere” developed by us [7] predicts the following time profile of the thermal desorption rate for the isothermal thermal desorption of excess oxygen from the bulk of the grain, when chemical reactions and phase transitions are absent (the rate-determining step is the diffusion of excess oxygen to the surface):

$$w(t) \approx (N_0/\pi^2\tau_D)(t/\tau_D)^{1/2} \exp(-t/\tau_D)^{1/2}, \quad (1)$$

$$\tau_D = a^2/4\pi^2D,$$

where  $N_0$  is the average amount of excess oxygen atoms in the oxide grain,  $a$  is the average radius of the oxide grain, and  $D$  is the diffusivity of excess oxygen in the oxide lattice.

However, the actual kinetics of atomic oxygen thermal desorption from the  $\beta\text{-Bi}_2\text{O}_3$  samples depends on their preparation procedure and history. A simple exponential character of the decay of the desorption intensity in the isothermal regime (Table 2, sample 4) was found for the fine-crystalline  $\beta\text{-Bi}_2\text{O}_3$ . As mentioned above [10], the hydration of  $\beta\text{-Bi}_2\text{O}_3$  powder by storing in a wet air or wetting the sample with distilled water followed by drying at  $T \approx 120^\circ\text{C}$  results in a substantial increase in the amount of desorbed atomic oxygen. The kinetics of thermal desorption decay under isothermal conditions is also exponential and the activation energy is extremely high (Table 2, sample 6). This fact can be explained by the possible recombination of a fraction of the hydroxyls introduced by hydration according to the following scheme as it shown in our previous work [10]



followed by the reaction

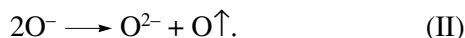


**Table 2.** The results of the measurements of atomic oxygen thermal desorption from bismuth oxides in the isothermal regime

Sample	Temperature of desorption, $^\circ\text{C}$	Amount of desorbed atoms $\text{O}^*$ , $\text{g}^{-1}$	Law of desorption rate decrease	Diffusivity, $\text{cm}^2/\text{s}$	Activation energy, $\text{kcal/mol}$
4	390	—	—	—	19.4
	425	$1.7 \times 10^{14}$	Exponent	—	
	480	$2.6 \times 10^{14}$	”	—	
5	390	—	—	$1.2 \times 10^{-13}$	30
	430	$3.6 \times 10^{12}, 2.8 \times 10^{13}$	$\exp(-k\sqrt{t})$	$3 \times 10^{-13}$	
	470	$3 \times 10^{12}, 7.2 \times 10^{13}$	”	$1.4 \times 10^{-12}$	
	490	$1.1 \times 10^{12}, 1.3 \times 10^{13}$	”	$1.8 \times 10^{-12}$	
6	480	—	—	—	40.7
	490	—	—	—	
	530	$10^{16}$	Exponent	—	

\* Sample 5: two figures correspond to the oxygen amount in two desorption peaks (see Fig. 2).

In both cases (fine-crystalline  $\beta\text{-Bi}_2\text{O}_3$  or hydrated sample), the simple exponential kinetics of the thermal desorption decay that does not correspond to Eq. (1) was found. It follows that diffusion is likely complicated by a chemical side reaction of the first (or pseudo-first) order, which is the rate-determining step of the whole process (it is this chemical side reaction that is characterized by the activation energy obtained for these samples). This conclusion is also confirmed by experimental data on the linear heating of fine-crystalline and hydrated  $\beta\text{-Bi}_2\text{O}_3$  samples. We have shown previously [10] that a weight loss of the sample occurs at temperatures up to  $500^\circ\text{C}$ , which are significantly higher than the temperature of the  $\beta \rightarrow \alpha$  transition ( $420^\circ\text{C}$ ). This weight loss is due to the removal of the structural  $\text{OH}^-$  groups (removal of excess oxygen from these samples of  $\beta\text{-Bi}_2\text{O}_3$  does not manifest itself on the DTA curves). Hence, the structural  $\text{OH}^-$  groups are maintained in the hydrated samples up to  $\sim 500^\circ\text{C}$ . Therefore, a small flow of O atoms, which is due to the desorption of excess oxygen from  $\beta\text{-Bi}_2\text{O}_3$  and accompanied by phase transition, is completely masked by a flow of oxygen atoms formed by reactions (I) and (II) over a wide temperature range.

The only sample on which the desorption flow in the isothermal regime obeyed Eq. (1) was  $\beta\text{-Bi}_2\text{O}_3$  prepared by precipitation from an aqueous solution (sample 5). After examining the thermal desorption kinetics for atomic oxygen from this sample, we attributed the first peak to the thermal desorption of atomic oxygen, which is located on the surface of oxide granules. The second peak concerns the thermal desorption of atomic oxygen, which diffuses from the granule bulk. A decrease in atomic oxygen desorption at high temperatures (Table 2, sample 5) is likely due to the concurrent recombinative desorption of atoms.

This is also confirmed by the experimental findings presented in Fig. 1. As can be seen, a decrease in atomic

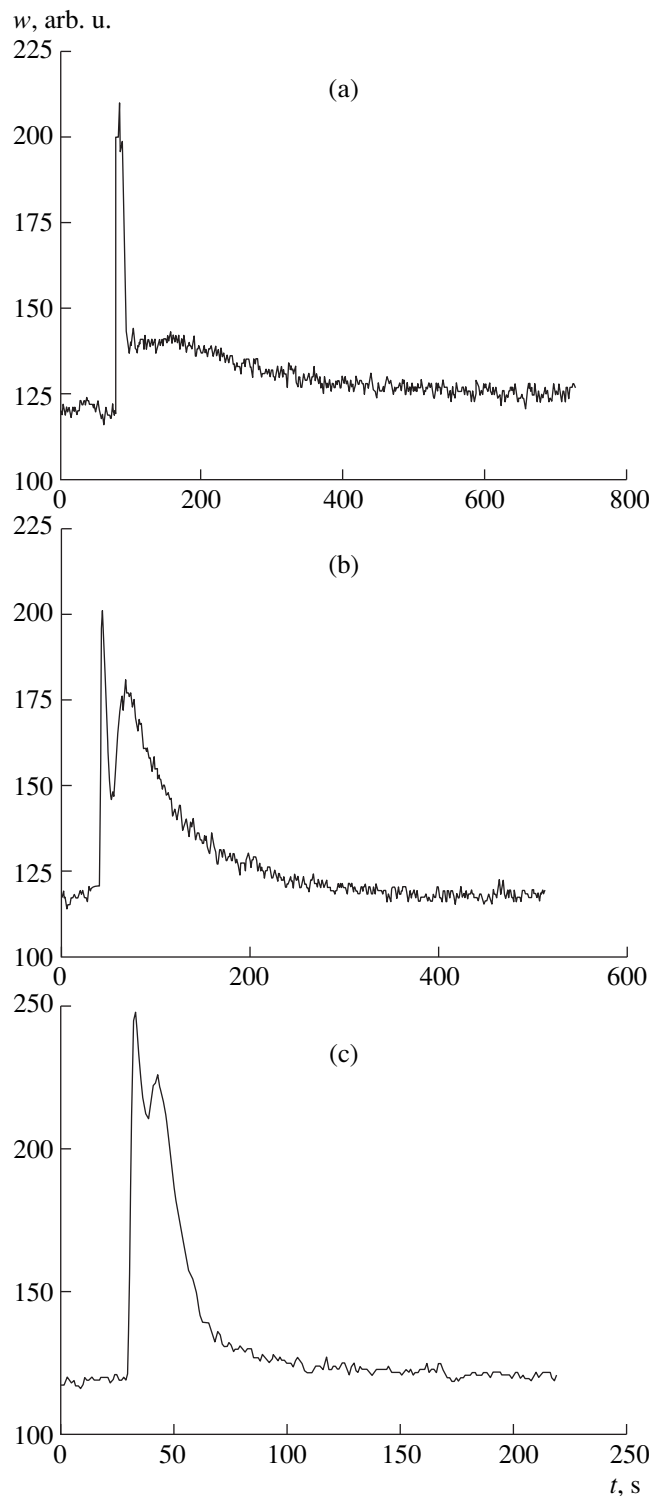


**Fig. 2.** Kinetics of atomic oxygen thermal desorption from  $\beta$ - $\text{Bi}_2\text{O}_3$  (sample 5) at temperatures,  $^{\circ}\text{C}$ : (a) 390, (b) 430, and (c) 490.

oxygen desorption is accompanied by an increase in the desorption of molecular oxygen, that is, the competitive oxygen desorption both in atomic and molecular forms takes place because both processes originate

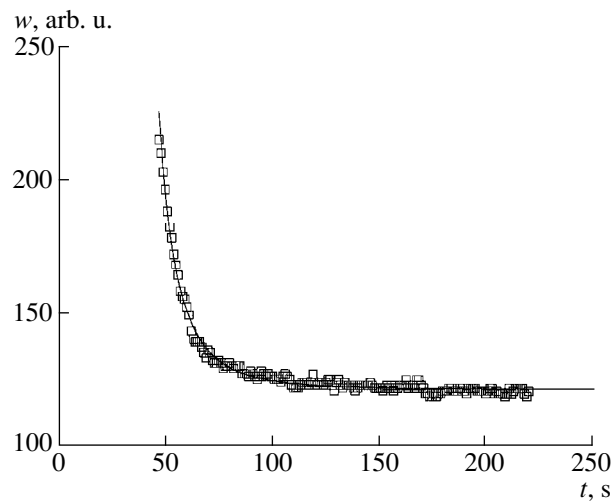


**Fig. 3.** Approximation of the kinetics of O thermal desorption at  $490^{\circ}\text{C}$  from sample 5 ( $\beta$ - $\text{Bi}_2\text{O}_3$ ) by theoretical Eq. (1). Points denote the experiment, and the curve denotes calculation.

from the diffusion of atomic oxygen from the grain bulk. The elucidation of a detailed mechanism requires additional experiments.

The above interpretation and the shape of curves (Figs. 2 and 3) follow from the “black sphere” model [7]. As it is seen from Fig. 3, the model satisfactorily describes the descending part of the second peak. The initial part of the second peak was ignored because the isothermal regime was not settled for such short times.

The problem on the rate-determining step of oxygen removal from the grain bulk is important because the use of the “black sphere” model suggests that the rate-determining step is oxygen diffusion from the bulk to the surface rather than the subsequent desorption. Let us consider this suggestion. A mathematical condition for the use of the “black sphere” model is the inequality

$$k_{\text{des}} > D/a^2,$$

where  $a$  is the average grain radius.

According to Frenkel:

$$k_{\text{des}} = 1/\tau = 10^{13} \exp(-Q/RT), \text{ s}^{-1},$$

where  $k_{\text{des}}$  is the rate constant of desorption,  $\tau$  is the lifetime of the adsorbed species, and  $Q$  is the heat of adsorption.

Taking the heat of adsorption of atomic oxygen on the surface of  $\text{Bi}_2\text{O}_3$  equal to  $\sim 44$  kcal/mol [11], we obtain at  $390^{\circ}\text{C}$ :  $k_{\text{des}} = 10^{13} \exp(-22000/663) = 2.8 \times 10^{-1} \text{ s}^{-1}$ , where  $Q/R = 22000$ .

At the same time, at  $D = 1.2 \times 10^{-13} \text{ cm}^2/\text{s}$  at  $390^{\circ}\text{C}$  (see Table 2) and the average grain radius of  $\sim 5 \times 10^3 \text{ \AA}$ ,  $D/a^2 = 1.3 \times 10^{-6} \text{ s}^{-1}$ , that is, the inequality is fulfilled with a confidence.

Thus, the rate-determining step in the atomic oxygen desorption from the sample of large-crystalline

$\beta$ -Bi<sub>2</sub>O<sub>3</sub> is the diffusion of atomic oxygen and, hence, the activation energies estimated from thermal desorption concern the atomic oxygen diffusion. One can also assume that O<sub>2</sub> desorption is partially the result of the recombination of atomic oxygen. In this case, taking into account the process energy, one can suggest that a fraction of desorbed O<sub>2</sub> can be vibrationally excited.

## CONCLUSIONS

(1) The main evolution of atomic oxygen from  $\beta$ -Bi<sub>2</sub>O<sub>3</sub> occurs at the expense of overstoichiometric lattice oxygen and is accompanied by the lattice reconstruction  $\beta$ -Bi<sub>2</sub>O<sub>3</sub>  $\longrightarrow$   $\alpha$ -Bi<sub>2</sub>O<sub>3</sub>.

(2) The "black sphere" model proposed by us earlier is valid in the case of excess oxygen diffusion not complicated by chemical side reactions. These conditions are fulfilled only for the large-crystalline sample in the absence of CO<sub>2</sub> and H<sub>2</sub>O, which form bismuth hydroxy-carbonates by interaction with fine-crystalline samples.

## REFERENCES

1. Che, M. and Tench, A.J., *Adv. Catal.*, 1982, vol. 31, p. 77; 1983, vol. 32, p. 2.
2. Martens, R., Gentsch, H., and Freund, F., *J. Catal.*, 1976, vol. 44, p. 366.
3. Zav'yalov, S.A., Myasnikov, I.A., and Zav'yalova, L.M., *Zh. Fiz. Khim.*, 1984, vol. 58, no. 6, p. 1532.
4. Yakunichev, M.V., Myasnikov, I.A., and Tsivenko, V.I., *Dokl. Akad. Nauk SSSR*, 1982, vol. 267, no. 4, p. 873.
5. Weng, L. and Delmon, B., *Appl. Catal.*, A, 1992, vol. 81, no. 1, p. 141.
6. Tsubo, T., Hiura, H., Horikawa, Y., and Shirasaki, T., *J. Catal.*, 1975, vol. 36, no. 2, p. 240.
7. Prostnev, A.S., Romanov, A.N., Rufov, Yu.N., *et al.*, *Khim. Fiz.*, 1996, vol. 15, no. 9, p. 148.
8. Romanov, A.N., Shashkin, D.P., and Khaula, E.V., *Zh. Neorg. Khim.*, 2000, vol. 45, no. 4, p. 554.
9. Romanov, A.N. and Rufov, Yu.N., *Zh. Fiz. Khim.*, 1996, vol. 70, no. 1, p. 171.
10. Romanov, A.N., Fattakhova, Z.T., and Rufov, Yu.N., *Khim. Fiz.*, 1998, vol. 17, no. 9, p. 85.
11. Kurumchin, E.Kh., in *Elektrodyne reaktsii v tverdykh elektrolitakh* (Electrode Reactions in Solid Electrolytes), Perfil'ev, M.V., Ed., Sverdlovsk: Ural. Otd., Akad. Nauk SSSR, 1990.